THE JOURNAL OF PHYSICAL CHEMISTRY B

Article

pubs.acs.org/JPCB

Nonfouling Hydrogels Formed from Charged Monomer Subunits

Sean C. Dobbins,[†] Daniel E. McGrath,[‡] and Matthew T. Bernards*[,†,‡]

[†]Departments of Chemical Engineering and [‡]Biological Engineering, University of Missouri, Columbia, Missouri 65211, United States

Supporting Information

ABSTRACT: A critical challenge in the field of biomaterials is the often undesirable, but immediate, coating of implants with nonspecifically adsorbed proteins upon contact with bodily fluids. Prior research has shown that overall neutral materials containing a homologous arrangement of mixed charges exhibit nonfouling properties. This has been widely demonstrated for zwitterionic materials and more recently for coatings containing an equimolar mixture of positively and negatively charged monomer subunits. In this investigation it is demonstrated that nonfouling hydrogels can be formed through this approach, and the physical properties of the resulting materials are thoroughly characterized. In particular, hydrogels were formed from mixtures of [2-(methacryloyloxy)ethyl]-trimethylammonium chloride (TM) and 3-sulfopropyl methacrylate potassium salt (SA) monomers with varying concentrations of a triethylene glycol dimethacrylate (TEGDMA) cross-linker. The swelling, weight percentage water, surface zeta potential, and compressional properties of the gels were characterized, and the nonfouling properties were demonstrated using enzyme-linked immunosorbant assays for both negatively charged fibrinogen and positively charged lysozyme. The results confirm that the TM:SA hydrogel systems have nonfouling properties that are equivalent to established nonfouling controls. Additionally, even though the gels were resistant to nonspecific protein adsorption, a composition analysis suggests that there is room to further improve the nonfouling performance because there is a slight enrichment of the SA monomer relative to the TM monomer.

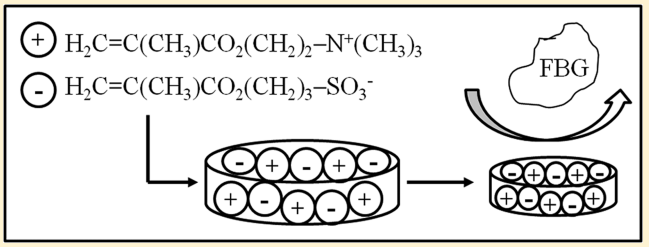

1. INTRODUCTION

Nonfouling materials are of great interest to the biomaterials community for tissue engineering, drug delivery, and biosensor platform applications. Therefore, a number of investigators have pursued functional groups that reduce or eliminate nonspecific protein adsorption. The most widely investigated materials come from the PEG family of molecules.[1−3] Tunable PEG-based hydrogel systems are well characterized as drug delivery systems[4,5] and as tissue engineering scaffolds,[6] among other applications.[7] While PEG-based materials are widely used, they have not completely solved the issue of nonspecific protein adsorption in the complex *in vivo* environment, possibly because they are subject to oxidation in biochemically relevant solutions.[8−10]

The next most widely investigated family of nonfouling functional groups is zwitterionic materials that contain a positively charged and negatively charged moiety within a single pendant group.[11−14] Examples of these materials include phosphorylcholine (PC), sulfobetaine (SB), and carboxybetaine (CB) based chemistries. Zwitterionic functional groups have also been used to form hydrogel materials for multiple biomedical applications.[15−18] More recent efforts with zwitterionic based hydrogels are focused on improving the mechanical properties of the hydrogel through chemical modifications to the cross-linker molecules.[19] While these materials have shown good promise as nonfouling hydrogels, the final material properties are ultimately dictated by the underlying monomer, and this is a drawback given the wide range of applications where nonfouling properties are of interest.

Molecular dynamics simulations have suggested that the nonfouling properties of PEG and PC based materials are derived from the formation of a strong hydration layer immediately adjacent to the functional groups. In the case of PEG this hydration layer is formed through hydrogen bonding, and in the case of PC it is formed through ionic solvation interactions.[20,21] These results have been supported by experimental investigations to quantify and characterize this hydration layer in both PEG and SB based materials, among others.[22−24]

It has been suggested that mixed charge or polyampholyte systems would have similar nonfouling properties to their zwitterionic counterparts. This was first demonstrated with self-assembled monolayer (SAM) systems.[10] Our previous work demonstrated that this concept could be applied to polyampholyte statistical copolymer brushes. These polymer brush coatings have been demonstrated to be nonfouling, as long as the individual charged units were homogeneously mixed at the molecular level.[25−27] This approach has since been adapted by others in additional polymer brush systems.[28−30] Similarly, investigators have examined polyampholyte polymer coatings that are adsorbed to surfaces rather than being grafted from the surface as an alternative mechanism for creating nonfouling surface coatings.[31,32]

Received: July 31, 2012
Revised: November 19, 2012
Published: November 28, 2012

Polyampholyte hydrogels and microgels have also been widely investigated as temperature and/or pH responsive systems useful for carrying and delivering drugs and proteins.[33−36] Given this application, it is often desirable for the hydrogel system to have protein adsorption capabilities. For example, Denis et al. looked at the adsorption and desorption characteristics of bovine serum albumin (BSA) from a polyampholyte microgel and found that the desorption characteristics were dependent upon the electrolyte content of the media.[33] However, to date there has been very limited work to develop nonfouling polyampholyte hydrogel systems for biomaterial applications.[37] In one previous investigation, the resistance to nonspecific protein adsorption was only demonstrated for negatively charged fibrinogen (FBG). This lead to an incomplete investigation because previous work with polyampholyte materials clearly demonstrated that positively charged lysozyme (LYZ) can strongly adsorb to polyampholyte materials that have an enrichment of the negatively charged monomers.[26] Additionally, there have been no characterizations of the properties of the hydrogels beyond nonfouling which limits the ability to apply this approach to biomedical applications.[37]

In this study, hydrogels were created from mixtures of positively charged [2-(methacryloyloxy)ethyl]-trimethylammonium chloride (TM) and negatively charged 3-sulfopropyl methacrylate potassium salt (SA) monomers using triethylene glycol dimethacrylate (TEGDMA) as a cross-linker. The structures of these molecules can be seen in Scheme 1.

Scheme 1. Chemical Structures of the Monomers and Cross-Linker Used in This Investigation

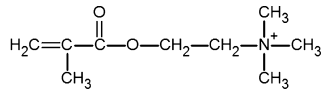

[2-(methacryloyloxy) ethyl] trimethyl ammonium chloride (TM)

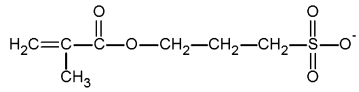

3 sulfopropyl methacrylate potassium salt (SA)

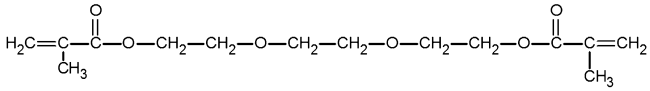

triethylene glycol dimethacrylate (TEGDMA)

The advantage to this approach is the hypothesis that the material properties can be controlled through monomer selection. However, the base case properties must first be developed. Therefore, the swelling, water content, surface zeta potential, and mechanical properties of the resulting TM:SA hydrogels were characterized as a function of the cross-linker concentration. Additionally, the nonfouling properties were characterized for both FBG and LYZ, and the chemical compositions were determined. The results demonstrate that TM:SA polyampholyte hydrogel materials have nonfouling properties that are on par with other established nonfouling chemistries across a range of cross-linker densities, with room for further improvement through increased control over the polymerization chemistry.

2. MATERIALS AND METHODS

2.1. Materials. Phosphate buffered saline powder (150 mM, pH 7.4), TM, SA, TEGDMA, and LYZ from chicken egg white (≥90%) were purchased from Sigma-Aldrich (St. Louis, MO). *N*-(3-Sulfopropyl)-*N*-methacryloxyethyl-*N*,*N*-dimethylammonium betaine (SBMA) was purchased from Monomer-Polymer and Dajac Laboratories (Trevose, PA). Ammonium persulfate (APS) was purchased from Acros Organics (Pittsburgh, PA). Ethylene glycol and sodium metabisulfite (SMS) were purchased from Fisher Scientific Inc. (Pittsburgh, PA). FBG from human plasma (100%) was purchased from EMD Biosciences (San Diego, CA). Horseradish peroxidase (HRP)-conjugated polyclonal antifibrinogen (human plasma) and HRP-conjugated polyclonal antilysozyme (chicken egg white) were purchased from United States Biological (Swampscott, MA). Ethanol was purchased from Decon Laboratories, Inc. (King of Prussia, PA). Deionized (DI) water was obtained from a Millipore Elix water purification system (Billerica, MA) and used for all experiments.

2.2. Hydrogel Synthesis. The hydrogel synthesis procedures were adapted from previous related work.[37] Briefly, TM:SA hydrogels were created by mixing 1 mmol of TM with 1 mmol of SA and the volume of TEGDMA of interest in 500 μL of solvent solution consisting of H_2O, EtOH, and ethylene glycol in a 1.5:1:1.5 ratio. Three cross-linker concentrations were investigated in this study: 0.075 mmol (1×), 0.15 mmol (2×), and 0.30 mmol (4×) of TEGDMA, resulting in total monomer to cross-linker ratios of 26.7:1 (1×), 13.3:1 (2×), and 6.7:1 (4×). Polymerization was initiated using 8 μL of a 40% (w/w) APS solution in DI H_2O and 8 μL of a 15% (w/w) SMS in DI H_2O. The reaction mixture was placed between two glass microscope slides, separated by a polytetrafluoroethylene spacer with thickness of 0.79 mm, and placed in an oven at 60 °C for 1 h. The gels were then left to cool for at least 1 h at room temperature before investigation. The procedures to form pure TM and SA hydrogels were identical to the TM:SA hydrogels with the exception that 2 mmol of only one monomer was used. SB methacrylate (SBMA) hydrogels were created by mixing 2 mmol of SBMA with 20 μL of TEGDMA in 500 μL of a solvent solution consisting of H_2O and ethylene glycol in a 1:1 ratio. All other polymerization conditions were identical to the TM:SA procedures.

2.3. Equilibrium Swelling and Hydration Studies. Freshly prepared gels were cut into square sections with a lateral surface area of 1 cm^2. These samples were then placed into either DI H_2O or PBS solution (replaced daily) and monitored daily over a period of 8 days. Each day, the samples were briefly removed and their dimensions were measured. The percent area swelling was determined based on the ratio of the initial measured lateral surface area and the measured lateral surface area at each time point, expressed as a percentage. The error associated with these measurements is represented by the accuracy of the measurement technique because replicate experiments yielded identical results.

To measure the hydration levels, freshly prepared gels were allowed to soak overnight in PBS solution to fully equilibrate the samples. Then the gels were removed from the buffer and the surfaces of the gels were gently patted dry with tissue wipes to remove as much free surface water as possible. The gels were then weighed and placed in a desiccator containing Drierite (W.A. Hammond Drierite Company, Xenia, OH) under slight vacuum. The weight changes were monitored and found to

dx.doi.org/10.1021/jp307588b | J. Phys. Chem. B 2012, 116, 14346−14352

stabilize within 1 week. At that point the final sample weight was measured. The percent hydration was determined based on the change in weight relative to the initial sample weight. Both the swelling and hydration studies were conducted on three independently prepared samples (n = 3).

2.4. Zeta Potential Measurements. TM:SA (1×, 2×, and 4×) and SBMA hydrogel samples were prepared using the procedures above, and they were soaked overnight in DI water. The samples were then cut to fit into a flat sample zeta potential measurement cell for use with a DelsaNano HC instrument (Beckman Coulter, Brea, CA). The flow cell was thoroughly flushed with DI water, and then a 0.01 M NaCl solution, pH 7.4, containing a standard particle for flat surfaces tracer solution (Otsuka Electronics Co., Japan) was injected into the flow cell (1:200 nanoparticle:buffer ratio). The surface was allowed to stabilize for 15 min, and then the zeta potential was measured at 10 separate locations on each sample. This measurement was repeated three times. The average zeta potential for the sample was calculated and directly recorded by the instrument. As a control, identical experiments were conducted with a poly(methyl methacrylate) (PMMA) calibration control (Beckman Coulter). This control has a stated zeta potential of −16.3 ± 10.0 mV, and a value of −16.4 mV was recorded using these procedures.

2.5. Enzyme-Linked Immunosorbant Assay (ELISA) Studies. One TM:SA gel and one SBMA gel were created as described above. Following the room temperature cooling step, the gels were removed from the mold and placed in PBS solution to soak overnight to remove the initiators and any unreacted monomers. This overnight soak also allowed the samples to swell to their equilibrium size. The following day, each gel was punched into six 5 mm disks using a biopsy punch, and the disks were soaked again in fresh PBS solution overnight. Each set of gel disks were further divided into two groups. One group of TM:SA disks and SBMA disks were incubated in a 1 mg/mL solution of FBG in PBS. The other group of TM:SA disks and SBMA disks were incubated in a 1 mg/mL solution of LYZ in PBS. Additionally, three wells of a 24-well tissue culture polystyrene (TCPS) well plate were incubated in FBG, and three wells were incubated in LYZ to serve as positive fouling controls. A protein adsorption time period of 1.5 h was used. Following adsorption, the well plate and all of the hydrogel disks were washed five times with PBS solution. The disks and wells that were previously incubated in FBG were then incubated in 10 μg/mL HRP-conjugated anti-FBG, while the disks and wells that were previously incubated in LYZ were incubated in 10 μg/mL HRP-conjugated anti-LYZ. Again, a protein adsorption time period of 1.5 h was used. The hydrogel disks and wells were then washed five times with PBS solution. The individual hydrogel samples were then placed into separate clean wells in the well plate, and 800 μL of a substrate solution containing 0.1 M citrate−phosphate buffer (pH 5.0) with 0.03% hydrogen peroxide and 0.1 g of o-phenylenediamine was added to each well, including the TCPS fouling controls. The plate was then immediately placed into a BioTek PowerWave XS2 multiwell plate reader (Winooski, VT). The absorbance was measured at 492 nm at regular intervals over the course of 30 min using Gen5 1.07 software (BioTek). The relative levels of adsorbed proteins were determined based on the final signals for each well after 30 min. The final signals for each group of disks were averaged together and normalized to the averaged final signal for TCPS. These averages were obtained from each of three independent trials for each cross-linker density investigated (n = 9). Propagation of experimental uncertainty was conducted throughout all of the trials, and it was used to represent the error in the experimental data.

2.6. Compression Strength Testing. TM:SA samples were synthesized using similar procedures to those discussed above, with proportionally larger volumes. The solutions were placed into 15 mL centrifuge tubes instead of the glass slide molds and placed in the oven at 60 °C for 1 h. The samples were then removed from the oven and left to cool for 1 h. Then the samples were removed from the centrifuge tubes and soaked in PBS solution overnight. The next morning, the samples were cut into cylinders with a diameter of 1.8 cm and a length of 1 cm for immediate compression testing using a TAHDi Texture Analyzer (Texture Technologies Corp, Scarsdale, NY), equipped with a 5 kg load cell. A compression rate of 2 mm/s was used. The samples were compressed to fracture, and the stress and strain were tracked. The fracture stress and strain were determined as the maximum values measured before fracture. The elastic modulus was determined as the slope of a linear fit to the stress−strain curve over the 0−0.1 strain ratios. Three independently prepared samples were tested for each TM:SA cross-linker concentration (n = 3).

2.7. Composition Analysis. Hydrogel samples were prepared as discussed above. However, the samples were fully equilibrated in DI water rather than PBS to reduce the presence of ions in the samples. Following the overnight water soak, the samples were placed in a desiccator for a minimum of 7 days to fully dehydrate the samples. Then the samples were loaded into a Kratos Axis 165 photoelectron spectrometer (XPS) (Kratos Analytical, Inc., Chestnut Ridge, NY). XPS spectra were collected using a monochromatized Al Kα source with a source energy of 1486.6 eV, a spot size of ∼700 μm, and a takeoff angle of 60°. Kratos Vision Processing software was used to determine the peak areas, which were then used to determine the elemental compositions of the samples. The peak areas were normalized by the number of scans, points/electronvolt, Scofield photoionization cross section, and sampling depth for this calculation. Three independently prepared samples were analyzed for each cross-linker density and for the SBMA control (n = 3).

3. RESULTS AND DISCUSSION

3.1. Hydrogel Physical Characterizations. In order to accurately compare the nonfouling characteristics of multiple samples using ELISA, it is necessary to first determine the equilibrium swelling properties of the hydrogels. This allows for samples with identical surface areas to be compared, eliminating the need for normalization. The hydrogel equilibrium swelling studies were initiated with partially hydrated samples because of the presence of water in the polymerization solvent and the overall purpose of determining the final equilibrium size. The swelling characterization studies revealed that all of the hydrogel samples swelled to their maximum size within 1 day, with no quantifiable size change thereafter. These results are summarized in Table 1. As expected, it was found that the swelling was inversely related to the cross-linker density in both PBS and water. It can also be seen that for a given TM:SA cross-linker density the swelling ratio in water was always greater than in PBS. This is believed to be due to the presence of ions in PBS, which can interact with and neutralize the charged regions within the hydrogel. At the 4× cross-linker concentration, no swelling was found in the TM:SA gels in

Table 1. Physical Characteristics of TM:SA Hydrogels with Varying Cross-Linker Densities at Equilibrium

	cross-sectional area swelling[a] (%)			
sample	H_2O	PBS	hydration (wt %)	zeta potential (mV)
1× TM:SA	324 ± 1	196 ± 1	85.0 ± 1.0	−1.93
2× TM:SA	225 ± 1	169 ± 1	79.6 ± 4.0	−2.65
4× TM:SA	100 ± 1	100 ± 1	69.7 ± 1.8	+0.28
SBMA control	144 ± 1	196 ± 1		−0.85

[a]The error ranges provided for the cross-sectional area swelling results represent the accuracy of the experimental measurements because three replicate experiments yielded identical results.

either PBS or water. The equilibrium swelling characteristics of the zwitterionic analogue SBMA are also summarized in Table 1. It is interesting to note that the swelling of SBMA is higher in PBS than in water, and this is attributed to differences in the distribution of the charged groups as compared to the TM:SA samples (separate side chains versus a single side chain). The swelling studies were also remarkably reproducible as the results across replicate samples (n = 3) were identical based on the accuracy of the measurement technique.

The nonfouling properties of hydrogel materials are believed to be dependent upon the formation of a strongly bound hydration layer along the surface. The equilibrium hydration weight percent was determined to compare the water content of the different hydrogel cross-linker densities, and the results are shown in Table 1. The highest water content was found for the TM:SA hydrogel with a 1× cross-linker density, where the average weight percent of water was 85%. As the cross-linker density is increased, there is a nearly linear decrease in the water weight percent, to a 70% level for the 4× cross-linker density.

It is also possible that surface charge accumulation on the hydrogel surfaces can impact the nonspecific adsorption of proteins. The zeta potential of the surface was measured at pH 7.4 to determine the relative levels of surface charge. The results are presented in Table 1. As a neutral control, a PMMA calibration surface was also characterized and yielded a zeta potential of −16.4 mV at the test pH of 7.4. It was found that the TM:SA hydrogel samples across all three cross-linker densities were less than ±3.0 mV. Similarly, the zeta potential of the zwitterionic SBMA control was also less than −1.0 mV. These results are all less than the calibration range for the neutral PMMA control (±10.0 mV), suggesting that there is little to no surface charge on any of the hydrogel samples after the surfaces are allowed to reach their equilibrium state at this pH value.

In addition, the mechanical properties of the gels under compression were characterized. Figure 1 shows a representative compressional stress−strain curve for each of the cross-linker densities that were investigated here. The average mechanical properties that were obtained for the TM:SA hydrogels are summarized in Table 2. As expected, the compressional strength of the materials is noticeably increased as a function of cross-linker density. However, there is a related decrease in the elasticity of the gels. A maximum fracture stress of 146.0 ± 4.9 kPa was found for the TM:SA hydrogels with a 4× cross-linker density, which is suitable for some biomedical applications.

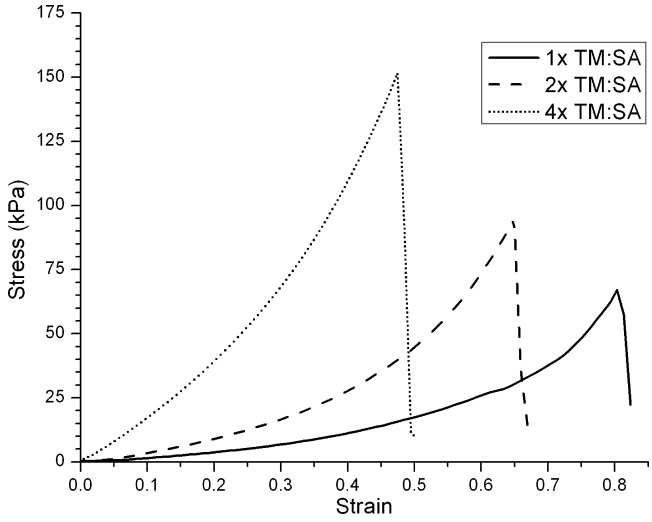

Figure 1. Representative compressional stress−strain curves for TM:SA hydrogels with varying concentrations of TEGDMA cross-linker.

3.2. Nonfouling Characterization. The nonfouling properties of the TM:SA hydrogels were demonstrated with both negatively charged FBG and positively charged LYZ using ELISA techniques. Because ELISA is qualitative, all of the results were normalized to a fouling control TCPS, which was considered to have a complete monolayer of adsorbed protein. This is a typical approach for comparing the nonspecific protein adsorption on different samples using ELISA.[38,39] SBMA hydrogels were included in the ELISA investigations as a known nonfouling control,[37,40] and hydrogels formed by the individual TM and SA monomers themselves were also investigated at a 1× cross-linker density. ELISA is both a time- and concentration-sensitive technique. Following the protein and antibody adsorption steps, the samples were exposed to the OPD substrate, and the responses were monitored over time. An example ELISA curve is shown in Figure 2a. The absorbance value was seen to reach a steady-state value for the TCPS controls for both FBG and LYZ within 30 min of analysis. This plateau suggests that the HRP enzymes present on these samples were able to react with a majority of the OPD substrate, limiting further reactions. In analyzing ELISA results, it is important to use the same substrate exposure time period for all of the samples under comparison because of the time dependence of the enzyme−substrate reaction. In Figure 2a, it is not readily apparent that there is a time dependence for the TM:SA and SBMA samples. Figure 2b shows the same curves with a reduced y-axis scale to demonstrate that they too vary as a function of time. However, the monitored ELISA response for both of these substrates is more linear in nature, suggesting that there are very few HRP enzymes present. These enzymes continually react with the OPD substrate because it is present in excess relative to the enzyme concentration. Based on the results seen in Figures 2a,b, a time point of 30 min was selected as the end point for all of the direct substrate comparisons.

The results of the ELISA experiments are summarized in Figure 3. As expected, the SBMA nonfouling control had nonspecific protein adsorption levels that were less than 6% of that seen on the fouling TCPS control for both FBG and LYZ. The TM:SA hydrogels performed nearly as well as the SBMA hydrogels, with protein adsorption levels less than 6% of that

dx.doi.org/10.1021/jp307588b | J. Phys. Chem. B 2012, 116, 14346−14352

Table 2. Mechanical and Chemical Properties of TM:SA Hydrogels with Varying Cross-Linker Densities

sample	fracture stress (kPa)	fracture strain	modulus (kPa)	S/N (at. %)
1× TM:SA	68.8 ± 3.6	0.77 ± 0.01	10.8 ± 2.0	1.90 ± 0.44
2× TM:SA	97.4 ± 4.2	0.59 ± 0.12	44.5 ± 36.9	2.86 ± 0.31
4× TM:SA	146.0 ± 4.9	0.42 ± 0.06	126.7 ± 42.8	2.23 ± 0.55
SBMA control				1.62 ± 0.49

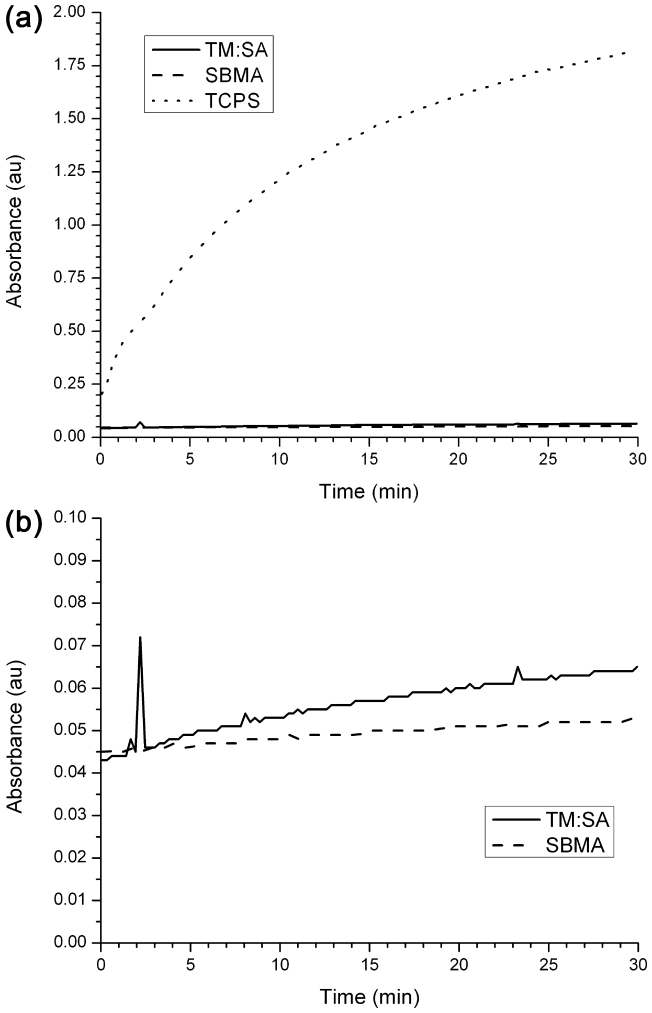

Figure 2. (a) Representative ELISA absorbance curves for TCPS, 1× TM:SA, and SBMA samples following exposure to LYZ, HRP-conjugated anti-LYZ, and OPD substrate. (b) The same ELISA absorbance curves for the 1× and SBMA samples shown with a smaller *y*-axis scale. The curves demonstrate both the time and concentration dependence of the measured ELISA response.

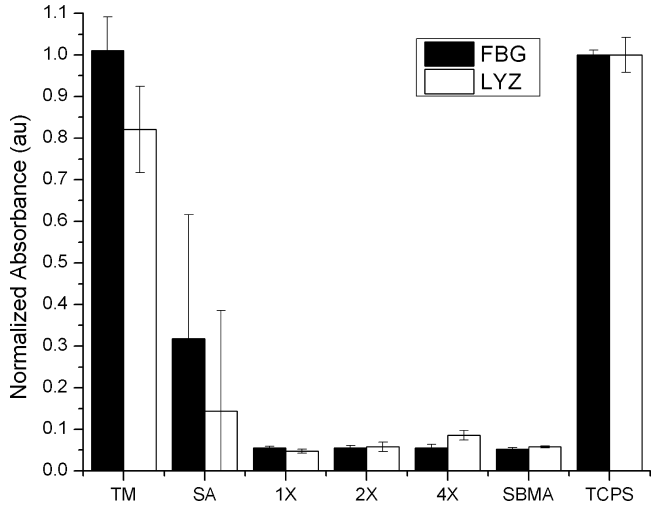

Figure 3. Mean ± propagated error of the nonspecific protein adsorption to various hydrogel substrates (n = 9). The results are presented as the absorbance measured following 30 min of exposure to OPD and normalized to the results for TCPS.

seen on TCPS for both FBG and LYZ across all of the cross-linker densities, with the exception of LYZ adsorption to the 4× cross-linker density. The 4× TM:SA hydrogels had a slightly higher level of adsorbed LYZ, at ~8.5% of that seen on TCPS. These results suggest that the TM:SA polyampholyte hydrogels have excellent nonfouling properties.

These results are even more promising when the nonspecific protein adsorption to hydrogels formed from the individual monomers is considered. As seen in Figure 3, there is an identical amount of FBG that adsorbs to the TM hydrogel as compared to the TCPS. Additionally, the adsorbed amount of LYZ is >80% of that seen on TCPS. The SA hydrogel performs better, but there is significantly more protein adsorption as compared to the polyampholyte hydrogels. These results support the conclusion that polyampholyte materials have nonfouling properties that are as good as those seen by their zwitterionic counterparts only when they are charge neutral at the molecular level.

3.3. Chemical Composition. It is interesting to note that the nonspecific adsorption of LYZ to the TM:SA hydrogels shows a slow, but noticeable, increase as the cross-linker density is increased. In order to better understand this trend, XPS was conducted to assess the composition of the hydrogel materials. XPS is a surface sensitive technique, but it is possible that there will be some surface rearrangement of the hydrogel during the dehydration process. Therefore, the XPS results are only interpreted with respect to the overall hydrogel composition, which is expected to be uniform throughout the sample based on the polymerization procedures used in this study. The results are presented as the ratio of the atomic percentage of sulfur to nitrogen in Table 2. Additionally, representative broad survey spectra for each sample can be found in the Supporting Information. If the TM and SA monomers are present is a 1:1 ratio, as needed for optimizing the nonfouling properties of the hydrogel, this ratio should have a value of 1. The only source for nitrogen in these materials is the TM monomer. However, sulfur can be provided by both the SA monomer and any SMS initiator molecules that are not removed from the hydrogel during the overnight soak. To test for SMS artifacts from the polymerization process, SBMA hydrogels were also characterized by XPS because the nitrogen and sulfur are naturally 1:1 in this zwitterionic hydrogel.

As seen in Table 2, the S:N ratio determined for the zwitterionic SBMA hydrogel is greater than 1. This suggests that there is residual SMS that remains within the hydrogel structure following the overnight DI water soak. It is possible that electrostatic interactions between the charged SMS

dx.doi.org/10.1021/jp307588b | J. Phys. Chem. B 2012, 116, 14346−14352

initiator and regions of the SBMA monomer prevent the complete removal of the initiator during the overnight water soak. In spite of this fact, the nonfouling properties were still clearly demonstrated, suggesting that the residual SMS does not impact this property. Additionally, the ratio of 1.62:1 should be used as the baseline for examining the composition of the TM:SA hydrogel samples to account for the residual SMS initiator. As seen in Table 2, the S:N ratio for the TM:SA hydrogels were all greater than the 1.62 baseline value determined for the SBMA hydrogel. While the ratios are not statistically significant from each other, they can be used to interpret qualitative differences between the hydrogel samples. The challenge with getting more accurate quantifications of the S:N ratio lies in the fact that these two elements account for less than 4% of the total number of elements that would be found in a 1:1 ratio of TM and SA monomers, even in the absence of the TEGDMA cross-linker.

The fact that all of the TM:SA hydrogels have an S:N ratio greater than that determined for SBMA suggests that in addition to residual SMS there is an enrichment of the SA monomer. The fact that there is SA enrichment suggests that the SA monomer has either faster polymerization kinetics or a more favorable polymerization overall, under the conditions utilized here, leading to greater levels of the SA monomer being present in the final sample. A similar SA enrichment was seen in our previous investigation examining TM:SA polymer brushes. In that study, different molar ratios of TM to SA were investigated to identify the optimal conditions for forming a nonfouling polymer brush coating. In two of the three monomer ratios tested, it was determined that there was slight SA enrichment in the final polymer composition as compared to the monomer ratio in the reaction solution.[26] Based on the measured surface zeta potential, however, there is not enough SA enrichment in these samples to cause a significant surface charge.

The fact that there is a slight SA enrichment at the surface may be used to explain why there is an increased level of LYZ adsorption to the TM:SA hydrogels, especially at the 4× cross-linker density. An enrichment of negatively charged SA monomers results in an overall negatively charged hydrogel, which will have an attractive electrostatic interaction with positively charged LYZ. The level of SA enrichment is similar across all of the cross-linker densities that were examined in this study based on both the XPS and zeta potential measurements. It is hypothesized that this slight attraction is counteracted by the formation of stronger hydration layers at the lower cross-linker densities, thereby resulting in better nonfouling properties. As the amount of hydrating water is decreased with increasing cross-linker concentration as shown in Table 1, these electrostatic attractions become more important, leading to the higher levels of LYZ adsorption seen in the 4× TM:SA samples. The slight surface charge does not impact the adsorption of FBG to the same extent as LYZ because FBG is oppositely charged at neutral pH. However, when the hydrogel sample is prepared with only SA monomers, and fully negatively charged, the FBG adsorption levels increase. FBG is widely known to adsorb strongly to a variety of substrates, and it is likely that it changes its conformation before adsorbing to the negatively charged SA hydrogel. This response is similar to that seen in our previous work with TM:SA polymer brush coatings. In the prior study, minimal FBG adsorption was measured on TM:SA polymer brushes formed from a 1:2 ratio of monomers, but significant FBG adsorption was measured on pure SA polymer brushes.[26] The results found in this study also suggest that there is room to improve the performance of the TM:SA hydrogels further by better controlling the polymerization chemistry, as all three cross-linker densities showed SA enrichment relative to the SBMA control. This is currently under investigation.

4. CONCLUSIONS

In this work polyampholyte hydrogels composed of mixtures of positively charged TM and negatively charged SA monomers were formed and fully characterized as a function of the cross-linker density. These materials were shown to have excellent resistance to nonspecific protein adsorption from both negatively charged FBG and positively charged LYZ. At the same time, the chemical compositions of the resulting hydrogels as measured by XPS indicated that there is slight enrichment of the SA monomer relative to the TM monomer. This suggests that the protein resistance of the final materials can be further improved even though they were already on par with the nonfouling control SBMA. This investigation confirms that polyampholyte hydrogels composed of TM and SA provide a promising platform for nonfouling applications.

■ ASSOCIATED CONTENT

Ⓢ Supporting Information

Representative XPS spectra for each TM:SA cross-linker density and the SBMA control. This material is available free of charge via the Internet at http://pubs.acs.org.

■ AUTHOR INFORMATION

Corresponding Author

*E-mail: bernardsm@missouri.edu.

Notes

The authors declare no competing financial interest.

■ ACKNOWLEDGMENTS

The authors acknowledge Dr. Fu-hung Hsieh and Harold Hess for their assistance with the compression testing and Brian Porter from the Materials Research Center at Missouri Science and Technology for assistance with the XPS characterization and Kevin Zurick and the Micro/Nano Technology Facility for assistance with the surface zeta potential measurements. This study was supported by a Richard Wallace Research Incentive Grant Award and by the MU College of Engineering.

■ REFERENCES

(1) Ma, H.; Hyun, J.; Stiller, P.; Chilkoti, A. *Adv. Mater.* **2004**, *16*, 338−341.
(2) Ma, H.; Li, D.; Sheng, X.; Zhao, B.; Chilkoti, A. *Langmuir* **2006**, *22*, 3751−3756.
(3) Ma, H.; Wells, M.; T. P., B., Jr.; Chilkoti, A. *Adv. Funct. Mater.* **2006**, *16*, 640−648.
(4) Zustiak, S. P.; Leach, J. B. *Biomacromolecules* **2010**, *11*, 1348−1357.
(5) Zustiak, S. P.; Leach, J. B. *Biotechnol. Bioeng.* **2011**, *108*, 197−206.
(6) Kloxin, A. M.; Kloxin, C. J.; Bowman, C. N.; Anseth, K. S. *Adv. Mater.* **2010**, *22*, 3484−3494.
(7) Hoffman, A. S. *Adv. Drug Delivery Rev.* **2002**, *54*, 3−12.
(8) Herold, D. A.; Keil, K.; Bruns, D. E. *Biochem. Pharmacol.* **1989**, *38*, 73−76.
(9) Li, L.; Chen, S.; Zheng, J.; Ratner, B. D.; Jiang, S. *J. Phys. Chem. B* **2005**, *109*, 2934−2941.
(10) Ostuni, E.; Chapman, R. G.; Liang, M. N.; Meluleni, G.; Pier, G.; Ingber, D. E.; Whitesides, G. M. *Langmuir* **2001**, *17*, 6336−6343.

(11) Feng, W.; Brash, J.; Zhu, S. *J. Polym. Sci., Part A: Polym. Chem.* **2004**, *42*, 2931−2942.
(12) Feng, W.; Brash, J. L.; Zhu, S. *Biomaterials* **2006**, *27*, 847−855.
(13) Feng, W.; Zhu, S.; Ishihara, K.; Brash, J. L. *Langmuir* **2005**, *21*, 5980−5987.
(14) Ladd, J.; Zhang, Z.; Chen, S.; Hower, J. C.; Jiang, S. *Biomacromolecules* **2008**, *9*, 1357−1361.
(15) Carr, L. R.; Xue, H.; Jiang, S. *Biomaterials* **2011**, *32*, 961−968.
(16) Chang, Y.; Chen, S.; Yu, Q.; Zhang, Z.; Bernards, M. T.; Jiang, S. *Biomacromolecules* **2007**, *8*, 122−127.
(17) Ishihara, K.; Nomura, H.; Mihara, T.; Kurita, K.; Iwasaki, Y.; Nakabayashi, N. *J. Biomed. Mater. Res.* **1998**, *39*, 323−330.
(18) Lewis, A. L. *Colloids Surf., B* **2000**, *18*, 261−275.
(19) Carr, L.; Cheng, G.; Xue, H.; Jiang, S. *Langmuir* **2010**, *26*, 14793−14798.
(20) He, Y.; Hower, J.; Chen, S.; Bernards, M. T.; Chang, Y.; Jiang, S. *Langmuir* **2008**, *24*, 10358−10364.
(21) Zheng, J.; Li, L.; Tsao, H. K.; Sheng, Y. J.; Chen, S.; Jiang, S. *Biophys. J.* **2005**, *89*, 158−167.
(22) Hower, J. C.; Bernards, M. T.; Chen, S.; Tsao, H.-K.; Sheng, Y.-J.; Jiang, S. *J. Phys. Chem. B* **2008**, *113*, 197−201.
(23) Stein, M. J.; Weidner, T.; McCrea, K.; Castner, D. G.; Ratner, B. D. *J. Phys. Chem. B* **2009**, *113*, 11550−11556.
(24) Hoffman, A. S. *J. Biomater. Sci., Polym. Ed.* **1999**, *10*, 1011.
(25) Tah, T.; Bernards, M. T. *Colloids Surf., B* **2012**, *93*, 195−201.
(26) Bernards, M. T.; Cheng, G.; Zhang, Z.; Jiang, S. *Macromolecules* **2008**, *41*, 4216−4219.
(27) Mi, L.; Bernards, M. T.; Cheng, G.; Yu, Q.; Jiang, S. *Biomaterials* **2010**, *31*, 2919−2925.
(28) Chang, Y.; Shu, S.-H.; Shih, Y.-J.; Chu, C.-W.; Ruaan, R.-C.; Chen, W.-Y. *Langmuir* **2009**, *26*, 3522−3530.
(29) Li, G.; Xue, H.; Gao, C.; Zhang, F.; Jiang, S. *Macromolecules* **2009**, *43*, 14−16.
(30) Herzberg, M.; Sweity, A.; Brami, M.; Kaufman, Y.; Freger, V.; Oron, G.; Belfer, S.; Kasher, R. *Biomacromolecules* **2011**, *12*, 1169−1177.
(31) Mahltig, B.; Werner, C.; Mullet, M.; Jerome, R.; Stamm, M. *J. Biomater. Sci., Polym. Ed.* **2001**, *12*, 995−1010.
(32) Xie, L.; Hong, F.; He, C.; Ma, C.; Liu, J.; Zhang, G.; Wu, C. *Polymer* **2011**, *52*, 3738−3744.
(33) Leal Denis, M. a. F.; Carballo, R. R.; Spiaggi, A. J.; Dabas, P. C.; Campo Dallâ€ Orto, V.; MartÃnez, J. M. L. z.; Buldain, G. Y. *React. Funct. Polym.* **2008**, *68*, 169−181.
(34) Tan, B. H.; Ravi, P.; Tam, K. C. *Macromol. Rapid Commun.* **2006**, *27*, 522−528.
(35) Tan, B. H.; Ravi, P.; Tan, L. N.; Tam, K. C. *J. Colloid Interface Sci.* **2007**, *309*, 453−463.
(36) Kanazawa, R.; Sasaki, A.; Tokuyama, H. *Sep. Purif. Technol.* **2012**, *96*, 26−32.
(37) Chen, S.; Jiang, S. *Adv. Mater.* **2008**, *20*, 335−338.
(38) Parker, A. P.; Reynolds, P. A.; Lewis, A. L.; Kirkwood, L.; Hughes, L. G. *Colloids Surf., B* **2005**, *46*, 204−217.
(39) Chang, Y.; Chang, Y.; Higuchi, A.; Shih, Y.-J.; Li, P.-T.; Chen, W.-Y.; Tsai, E.-M.; Hsiue, G.-H. *Langmuir* **2012**, *28*, 4309−4317.
(40) Cheng, G.; Zhang, Z.; Chen, S.; Bryers, J. D.; Jiang, S. *Biomaterials* **2007**, *28*, 4192−4199.